The effect of environment on peptide and protein folding

Xue, Ying

CHAPTER 5

The effect of polyethylene glycol (PEG) spacers on the conformational properties of small peptides: a molecular dynamics study.

Summary:

Polyethylene Glycol (PEG) is used as an inert spacer in a wide range of biotechnological applications. In particular PEG can be used to display peptide epitopes for diagnostic purposes such as micro array techniques. Using molecular dynamics (MD) simulation techniques, we have investigated the influence of the PEG spacer on the conformational properties of the peptides to which it is attached. A series of five peptides with differing physical-chemical properties have been examined. Based on an analysis of backbone φ/ψ angles and the relative populations of alternative conformations, it has been shown that when isolated in solution the PEG spacer had little effect on the conformation of the peptide to which it was attached. However, when constrained to a two dimensional lattice mimicking a peptide displayed on a surface, the PEG-peptide units aggregated dramatically reducing the accessibility of the peptides to solvent.

Ying Xue, Megan O'Mara, Peter Surawski, Matt. Trau, and Alan E. Mark. To be submitted.

5.1 Introduction.

Polyethylene glycol (PEG) is by far one of the most widely used polymer in aqueous solutions of biological molecules [2]. It composed of repeating $(CH_2CH_2O)_n$ units. Pure polyethylene glycol forms a wax like solid (molecular weight between 200-2000) or opaque white flakes (above 2000). It is soluble in a wide range of organic solvents such as benzene, chloroform, dimethylformamide (DMF), as well as in water [2, 3]. Due to its non-toxic, non-ionic and hydrophilic characteristics, the FDA has approved PEG for use in a wide variety of products ranging from a vehicle or base in foods and cosmetics to the covalent modification of peptide based pharmaceuticals [2]. The modification of a protein, peptide or non-peptidic molecule by the linking of one or more PEG chains (PEGylation) was first developed by Davis and colleagues in 1970's [2, 4, 5] and has become increasingly important over the last 20 years. Not only is PEG chemically inert but in aqueous solution it is heavily hydrated with each glycol subunit binding two to three water molecules. The excluded volume of PEG is between five and ten times that of a typical protein of similar molecular weight [2, 6] and as a consequence PEGylation can be used to shield peptides and proteins from electrostatic and hydrophobic interactions with other proteins or to reduce protein adsorption onto surfaces [7-11].

PEGylation can reduce the propensity for a protein to aggregate, and increase its solubility and stability [5, 12-15]. As a consequence, PEGylation can extend the time a protein will remain in circulation in the body and reduce immunogenicity. PEG can also be used as a linker to immobilize proteins or peptides on surfaces [16-19]. This can be done to functionalize a specific surface by coupling proteins such as enzymes or, to display peptide fragments to be recognized by antibodies or even whole cells. For example, Trau and colleagues [17-19] have used PEG to display antigenic peptide fragments on the surface of microspheres for diagnostic purposes. Such applications require that not only the peptide be accessible to a potential receptor such as an antibody but that the peptide is also able to adopt an appropriate conformation. The conformation of small peptides is known to be strongly dependent on their local environment. In the case of PEGylated peptides the conformation will also be affected by the nature of the covalent link. Although PEGylation is widely used to present peptides on surfaces little is known in regard to the extent to which the structural

properties especially of small peptides (5-10 a.a.) are affected by PEGylation.

The aim of this work was to understand the effect of PEG spacers on the conformational properties of small peptides to which they are attached. Specifically the conformation properties of a series of five peptides with differing physical-chemical properties in aqueous solution, attached to a PEG spacer in aqueous solution and attached to a two dimensional surface via a PEG spacer have been examined. The system was designed to mimic the microsphere environment recently developed by Trau and colleagues [17-19]. A range of properties have been compared including the backbone and side chain conformations and the relative populations of alternative conformations.

5.2 Methodology.

5.2.1 Force Field.

All MD simulations were performed using the GROMACS (Groningen Machine for Chemical Simulation) package, version 3.2.1 [20, 21]. The GROMOS 53A6 force field [22] was used to describe the peptides. The bond lengths, bond angles and non-bonded Lennard-Jones and Coulomb parameters of the PEG spacer were also taken from the GROMOS 53A6 force field. Two sets of torsion parameters were tested, one was taken from GROMOS 53A6 force field, and the other was based on *ab initio* calculations performed by Anderson and Wilson [23]. The simple point charge (SPC) water model [24] was used to describe the solvent water. Two alterative PEG spacers were examined. The first was PEG-10: R_1-(CH_2-CH_2-O-)$_{10}$-R_2, The second was three times longer, PEG-30: R_1-(CH_2-CH_2-O-)$_{10}$–CH_2-CH_2-CONH-R_3-(CH_2-CH_2-O-)$_{10}$-CH_2-CH_2-CONH-R_3-(CH_2-CH_2-O-)$_{10}$-R_2, where R_1 and R_3 correspond to ethyl groups. R_2 corresponds to a propyl group. To generate the peptide-spacer complex, the *C*-terminus of the peptide was covalently bound at the R_1 position of the PEG spacer (See Figure 5.1 (a)).

5.2.2 Systems.

Peptides.

To determine the effect of the PEG spacer on the conformational properties of small

peptides, a series of five peptides with differing physical-chemical properties were examined. An overview of the systems simulated is given in Table 5.1. The peptide YGSLPQ (systems I, II, III) is a specific epitome used by Trau *et al*. in experimental studies. As a range of experimental data were available for this sequence, it was used to examine the effects of N- and C-termini modifications in a PEGylated peptide. In system I, the N- and C-termini of YGSLPQ carried charges of NH_3^+ and COO^-, respectively. The N-terminus of YGSLPQ was charged in system II, while the C-terminus was blocked by the covalent attachment of a methylamino (-NH-CH_3) group. Both the N- and C-termini of YGSLPQ were neutralized in system III: the C-terminus was again covalently modified by the attachment of a methylamino group, while the N-terminus was acetylated (CH_3-CO-). The effect of PEGylation on a hydrophobic peptide (VFVVFV) and a polar peptide (GSGGSG), were examined in systems IV and V, respectively. Two PEGylated charged peptides were also studied: EEGEEG (system VI) and KKGKKG (system VII), were used to represent a negatively and a positively charged peptide, respectively.

PEG spacer.

System VIII consisted of an isolated PEG-10 molecule in solution and was used to investigate the ability of the force field to reproduce the structural properties of the PEG in isolation.

Peptide-PEG complexes.

Systems IX to XV involved a covalent complex between the peptide and the PEG polymer. The N-terminus of the peptide was protonated (NH_3^+) and the C-terminus was covalently bound to the PEG spacer via an amino ethyl link as shown in Figure 5.1 (a). System IX consisted of a single chain of YGSLPQ+PEG-10 in aqueous solution. System X was made up of a 3×3 array of YGSLPQ+PEG-10 strands. Systems XI to XV consisted of a 6×6 array of strands with each of the 5 peptides bound to a PEG-30 spacer. The 3×3 and the 6×6 arrays were fully periodic and designed to mimic the peptide when bound to the surface of a microsphere via a PEG spacer. Experimental evidence suggests that the surface loading of the microsphere is 0.5~0.6 μmol/g beads (Trau *et al.*, unpublished data). This corresponds to a surface

area of 3.24 nm^2 per strand or a distance of 1.8 nm between two adjacent strands. In systems X to XV, the terminal carbon of the propyl (R_1-group, see Figure 5.1 (a)) of the PEG spacer was harmonically restrained (K=5000 kJ mol nm^{-2}) to a square plannar lattice, as illustrated in Figure 5.1 (c). The distance between the adjacent terminal-carbon atoms was 1.8 nm. Note, as the diameter of the microsphere (6 μm) is more than 3,000 times greater than the distance between two adjacent PEG molecules, the effect of curvature in the system is negligible.

5.2.3 Simulation parameters.

All simulations were performed under periodic boundary conditions. In the case of isolated peptides, each peptide was placed in the center of a periodic rhombic dodecahedral box. The dimensions of the box in each case were chosen such that the minimum distance from any heavy atom of the peptide to the box wall was 1 nm. In the case of systems X to XV, the dimensions of the boxes, given in Table 5.1, were chosen such that the minimum distance to the box wall was 0.9 nm. This ensured that the system formed a continuous periodic lattice. The non-bonded interactions were evaluated using a twin-range method. Interactions within the shorter range cutoff of 0.9 nm were updated every step. Interactions within the longer range cutoff of 1.4 nm were updated every 5 steps together with the pair list. To minimize the effect of truncating the electrostatic interactions beyond the 1.4 nm long range cutoff, a reaction field correction was applied using a relative dielectric constant of ε_r = 78 [25]. The LINCS algorithm [26] was used to constrain the length of the covalent bonds in the peptide and PEG. The SETTLE algorithm [27] was used to constrain the geometry of the water molecules. In order to further extend the timescale that could be simulated, explicit hydrogen atoms in the peptide were replaced with dummy atoms, the positions of which were calculated each step based on the positions of the heavy atoms to which they were attached. This eliminates high frequency degrees of freedom associated with the bond angle vibrations involving hydrogens, allowing a time step of 4 fs to be used to integrate the equations of motion without affecting thermodynamic properties of the system significantly [28]. The MD simulations were carried out in the NPT-ensemble at T = 298 K, and P = 1 bar. The temperature was maintained close to the reference value by weak coupling to an external temperature bath [29], using a relaxation time constant of 0.1 ps. The pressure was maintained by

weak coupling to an external pressure bath, using a relaxation time constant of 0.5 ps. All systems were simulated using isotropic pressure coupling. Data were collected every 200 ps (0.2 ns) for analysis. Images were produced with the VMD program [30].

5.2.4 Cluster analysis.

The trajectories were clustered using the method of Daura *et al.* [31, 32]. First, a matrix of the positional root mean square deviation (RMSD) between all conformations was constructed. The conformation with the most neighbors within a specified cutoff was then determined. This structure (the center or representative configuration of the first cluster), together with all of its neighbors, were then removed from the ensemble and the procedure repeated to obtain the second and higher clusters until the set of structures was empty. In this work, two conformations were considered neighbors if the backbone between the two conformations RMSD was < 0.1 nm.

5.2.5 Ramachandran plots.

The backbone conformations of the peptide were analyzed in terms of the distribution of φ (C_{i-1}-N_i-$C\alpha_i$-C_i) and ψ (N_i-$C\alpha_i$-C_i-N_{i+1}) angles [1, 33]. The φ/ψ distributions (Ramachandran maps) were computed for the central four residues. The allowed regions for the non-glycine residues were taken to be: region I, -180°<φ<-30° and -80°<ψ<180°; region II, -30°<φ<90° and -10°<ψ<120°; region III: -180°<φ<-30° and -180°<ψ<-150° [34].

5.2.6 Side chains analysis.

The sampling of side chain conformations was analyzed by the comparing the free energy distributions around the χ^1 torsion angle N_i-$C^{\alpha}{}_i$-$C^{\beta}{}_i$-$C^{\gamma}{}_i$ [33] for the side chains. The χ^1 angles were binned using 10° windows and the relative free energy as a function of χ^1 was estimated as $\Delta G_{(\chi)} = - k_B T \ln[N_{A(\chi)}/N_{(\chi)}]$, where $N_{A(\chi)}$ is the number of samples within a given window and N is the total number of samples in all windows, k_B is the Boltzmann's constant and T is the temperature (298 K) [1].

5.2.7 RMSD matrix.

The RMSD matrix was calculated by performing a pair wise RMSD comparison of all structures in the combined trajectory after performing a least squares fit on all backbone atoms.

Table 5.1 An overview of the simulations.

System identifier	Model type	Num. molecules	Simulation time (ns)	Box dimensions (nm)	Num. water molecules
I	NH_3^+-YGSLPQ-COO^-	1	50	3.5×3.5×2.5	917
II	NH_3^+-YGSLPQ-CONH-CH_3	1	450	3.5×3.5×2.5	916
III	Ac-YGSLPQ-CONH-CH_3	1	50	3.5×3.5×2.5	913
IV	NH_3^+-VFVVFV-CONH-CH_3	1	450	3.7×3.7×2.6	1163
V	NH_3^+-GSGGSG-CONH-CH_3	1	450	3.4×3.4×2.4	895
VI	NH_3^+-EEGEEG-CONH-CH_3	1	450	3.4×3.4×2.4	906
VII	NH_3^+-KKGKKG-CONH-CH_3	1	450	3.8×3.8×2.7	1201
VIII	PEG-10	1	20	5.9×5.9×4.2	4797
IX	YGSLPQ + PEG-10	1	50	4.9×4.9×3.5	2765
X	YGSLPQ + PEG-10	3×3	50	5.4×5.4×6.0	5176
XI	YGSLPQ + PEG-30	6×6	12.5	10.8×10.8×9	30301
XII	VFVVFV + PEG-30	6×6	12.5	10.8×10.8×9	30158
XIII	GSGGSG + PEG-30	6×6	12.5	10.8×10.8×9	30738
XIV	EEGEEG + PEG-30	6×6	12.5	10.8×10.8×9	30310
XV	KKGKKG + PEG-30	6×6	12.5	10.8×10.8×9	30301

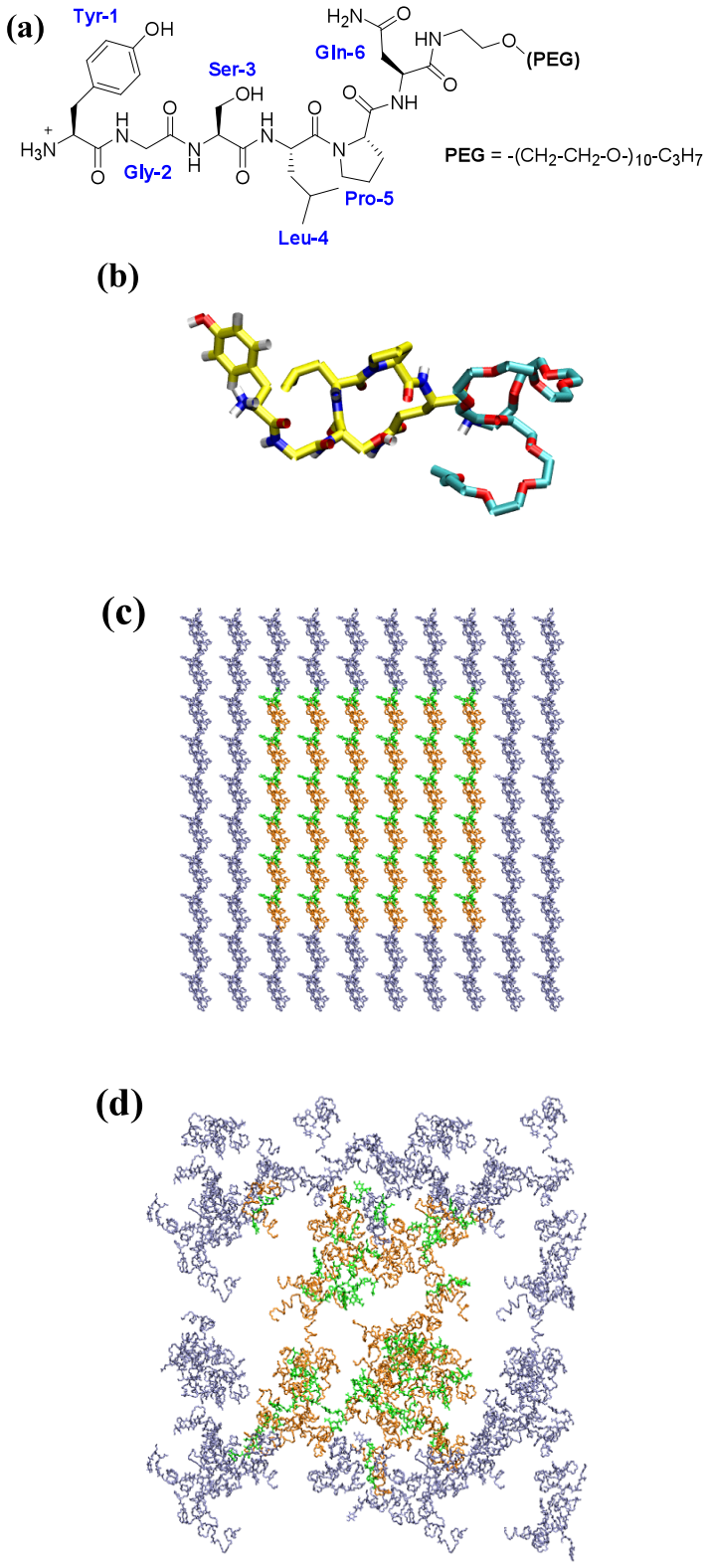

Figure 5.1 (a) The chemical structure of the peptide YGSLPQ covalently bound to a PEG-10 spacer. (b) The conformation of the YGSLPQ-PEG-10 in aqueous solution, after 5 ns of simulation (system IX)**.** (c) The initial configuration of a 6×6 array of YGSLPQ (brown)-PEG-30 (green) system XI. (d) System XI after 12.5 ns of simulation. Note, the central colored region corresponds to the simulation box. The blue region shows that under periodic conditions the system forms a continuous lattice.

5.3 Results and Discussion.

5.3.1 The conformation of the free peptide.

Structures of the peptide YGSLPQ were extracted from the 50 ns simulations of systems I, II and III and compared. Cluster analysis showed marked differences between the conformations sampled in the three systems. Figure 5.2 shows the predominant structure in each case. As can be seen from Figure 5.2 the nature of the end groups has a dramatic effect on the conformation of the isolated peptide. System I with charged termini, N-termini $–NH3^+$ and C-termini $–COO^-$, adopted primarily compact conformations (bent and turn conformations). In system II, N-terminus was charged ($-NH_3^+$) and the C-termini was blocked using a methylamino ($-NH-CH_3$) group, the conformations are less compact. In system III, the N-terminus was acetylated (CH_3-CO-) and the C-terminus again blocked using a methylamino ($-NH-CH_3$) group and the conformations sampled are predominately elongated. Clearly the differences in the electrostatic interactions due to the different termini dominate the conformational states sampled by the peptide.

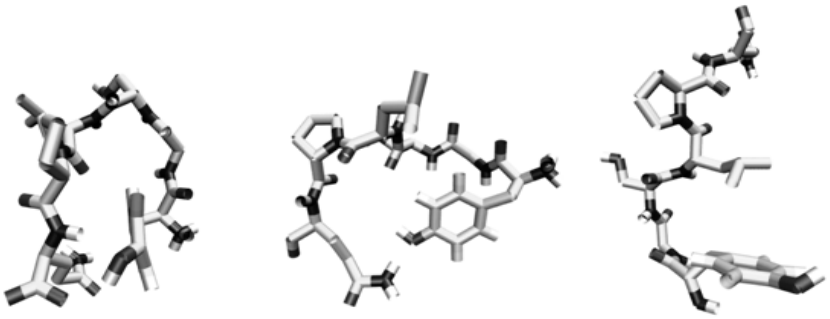

Figure 5.2 The dominant structure in the solution for the YGSLPQ peptide. (a) System I with charged termini, N-terminus $–NH3^+$ and C-terminus $–COO^-$. (b) System II, N-terminus NH_3^+ and the C-terminus was blocked using a methylamino ($-NH-CH_3$) group. (c) System III, the N-terminus was acetylated (CH_3-CO-) and the C-terminus again blocked using a methylamino ($-NH-CH_3$) group.

5.3.2 The conformation of PEG.

Before attempting to simulate the peptide linked to the PEG spacer, the structural properties of PEG in solution were analyzed. Experimental and theoretical studies suggest that PEG adopts a helical conformation in both a crystalline and an aqueous environment [23, 35-37]. In order to test the force field parameters used to describe the PEG spacer, a series of MD simulations of an isolated PEG molecule in water (system VIII) were performed. In these simulations, the PEG-10 was initially placed in a linear conformation. Using the dihedral parameters for the C-O-C-C, and O-C-C-O torsion angles taken from the GROMOS 53A6 parameter set, PEG did not adopt a helix but instead formed a random coil structure (results not shown). In contrast, using the dihedral parameters proposed by Anderson and Wilson for PEG based on *ab initio* calculations of a PEG monomer [23], the PEG adopted a helical conformation after about 5 ns. This conformation was stable in simulations of up to 20 ns (Figure 5.3). The parameters of Anderson and Wilson were used in all subsequent studies.

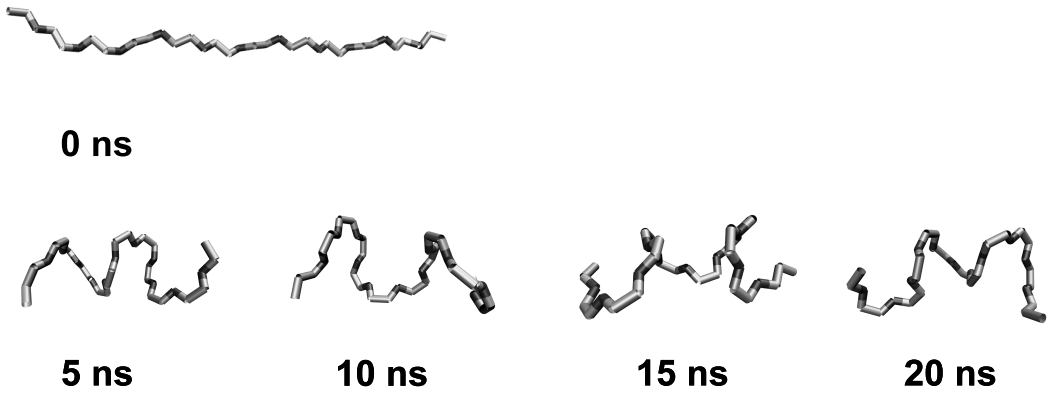

Figure 5.3 The conformation of PEG-10 in aqueous solution at 5 ns intervals from the simulation of system VIII.

5.3.3 The conformation of the peptide-PEG complex.

Figure 5.1 (b) shows a snapshot taken after 5 ns of simulation of the peptide YGSLPQ linked to the PEG-10 spacer in aqueous solution (system IX). As can be seen the PEG again rapidly adopts a helical conformation, the peptide attached to the PEG adopts primarily extended and turn conformations.

Figure 5.1 (c) and (d) show the initial (0 ns) and final (12.5 ns) configurations respectively of system XI, which consisted of an array of the peptide YGSLPQ, linked to the PEG-30 spacer in aqueous solution. As can be seen from Figure 5.1 (c), the initial configuration consisted of a regular array of the peptide YGSLPQ linked to the PEG-30 spacer. The initial conformation of the PEG-30 was an ideal helix. The peptide was modeled in an extended conformation. In the simulations there was a rapid collapse with the PEG-30 chains forming a range of irregular aggregates. The aggregate shown in Figure 5.1 (d) is typical of what was observed throughout the simulation. Note, the peptide linked PEG-30 spacers shown in Figure 5.1 (c) and (d) were restrained in the simulation to a 6×6 plannar square lattice with spacing of 1.8 nm between adjacent chains. This spacing was chosen to reproduce the average density of the peptide on a silica microsphere determined experimentally. In the simulations all 36 of the peptide linked polymers cluster together tightly suggesting the optimal local packing might be higher than the average value used in the simulations. In fact 36 units may be insufficient to represent the true nature of the clusters formed. Nevertheless, it is clear from the simulations that the peptide remains exposed to solvent. It was also observed that peptides attached to different PEG-30 chains readily interact at these packing densities. Initially in the simulation, several clusters formed with one pair of peptides forming a β-sheet structure. Most peptides, however adopted coil or turn conformations during the simulation.

5.3.5 The effect of PEG on the conformation of the peptide.

To investigate the possible effects of the PEG spacer on the conformation of the peptides to which they are attached, a series of four peptides with differing physical-chemical properties were examined in addition to the peptide YGSLPQ. These peptides were simulated either free in solution or attached to PEG spacer in a 2 D array system. In order to mimic the properties of a peptide attached PEG, in which the

N-terminus is protonated (NH_3^+) and the C-terminus is connected to the spacer, the peptides free in solution were modeled with the N-terminus protonated (NH_3^+) and the C-terminus blocked using a methylamino (-NH-CH_3) group. The simulations of free peptides in solution were each simulated for 450 ns so that the extent of sampling was equivalent to that of either the 3×3 (50 ns) or the 6×6 (12.5 ns) array systems.

5.3.5.1 The backbone conformation.

The φ/ψ distributions of the central four residues obtained from the 450 ns simulations of the isolated peptide systems, and the equivalent of 450 ns per peptide for the peptide-PEG complexes (either 9×50 ns or 36 ×12.5 ns) were compared. The φ/ψ distributions of the central four residues of the peptide YGSLPQ (Gly-2, Ser-3, Leu-4, and Pro-5) isolated in solution (system II) and an array of YGSLPQ+PEG-10 (system X) are plotted in Figure 5.4. The φ and ψ values in the allowed regions [34] are plotted as full circles, while those in the less favored regions are plotted as empty circles. As can be seen in Figure 5.4 the distributions of the φ/ψ values in system II and X are virtually identical. The primary difference is that for the three non-Gly residues, the proportion of structures outside the formally allowed regions was slightly higher in system X (2.77%) relative to system II (0.95%). Moreover, an equivalent degree of similarity the φ/ψ distributions between the isolated peptides and peptides attached to the PEG spacer was observed in all the other systems compared.

5.3.5.2 Side chain conformation.

The free energy distributions of the side chains for each residue as function of the χ^1 torsional angle were also calculated and compared. The curves overlapped closely in all cases. Figure 5.5 illustrates the result for the residue Tyr-1 in the isolated peptide YGSLPQ (system II) and a 6×6 array, YGSLPQ+PEG-30 (system XI). As can be seen in Figure 5.5 the curves for the isolated peptide (system II, solid line) superimpose on the curves for the peptide attached to the PEG spacer (system XI, dotted line).

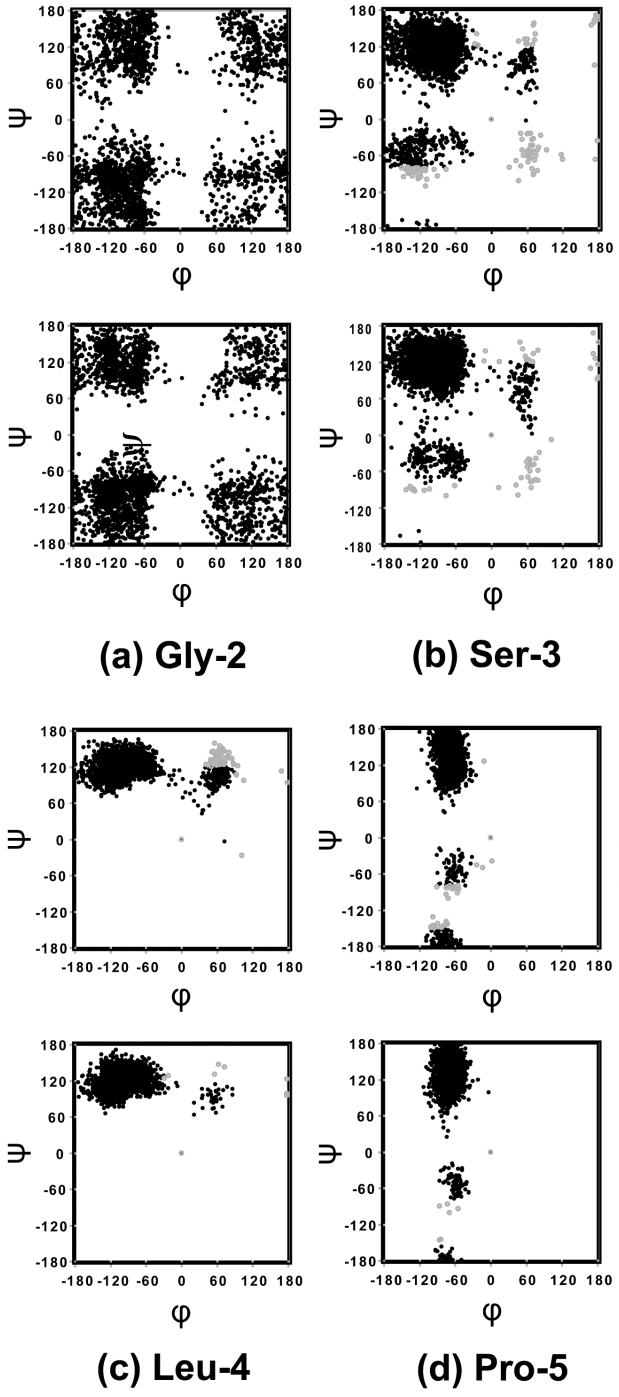

Figure 5.4 The Ramachandran distributions of residues (a) Gly-2, (b) Ser-3, (c) Leu-4, and (d) Pro-5 in the peptide YGSLPQ, obtained from the MD simulations of the peptide of in aqueous solution (system II, bottom panels) or covalently bound to a PEG-10 spacer (system X, top panels). The units of φ and ψ are degrees. For Ser-3, Leu-4 and Pro-5, φ and ψ angles in the allowed regions are plotted as black circles, while those in the disallowed regions are plotted as grey circles.

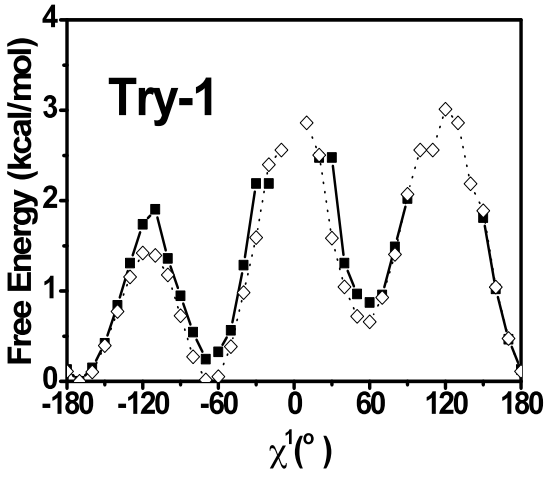

Figure 5.5. The distribution of the χ^1 dihedral angle of the sidechains of the YGSLPQ peptide residue Tyr-1 during the MD simulations. The free energy (potential of mean force) was obtained from the direct counting method [1]. The free energy curves for the system II: solid, the free energy curves for the system XI: dotted.

5.3.5.3 Cluster analysis.

For each type of peptide, all 4500 peptide configurations obtained from both simulations (half from isolated peptide and half from the peptide attached to the PEG-spacer) were combined and clustered based on the backbone RMSD. The first 10 clusters occupied about 90% of the ensemble.

The results for the peptide VFVVFV (system IV) and a 6×6 array of VFVVFV+PEG-30 (system XII) are shown in Figure 5.6. As can be seen from Figure 5.6, there is a high correlation between the proportion of configurations in each cluster consisting of the free peptide and the PEGylated peptide. The correlation coefficient was 0.95 and covariance 0.0026 for the first 10 clusters. The peptide adopts primarily extended and loose turn conformations during both simulations. Similar results were obtained for the other polar peptide as shown in Table 5.2. The two peptides containing charged side chain EEGEEG (negative charged) and KKGKKG (positive charged) show a poor correlation between the configurations sampled by the free peptide and the PEGylated peptide (0.32 and 0.64 respectively).

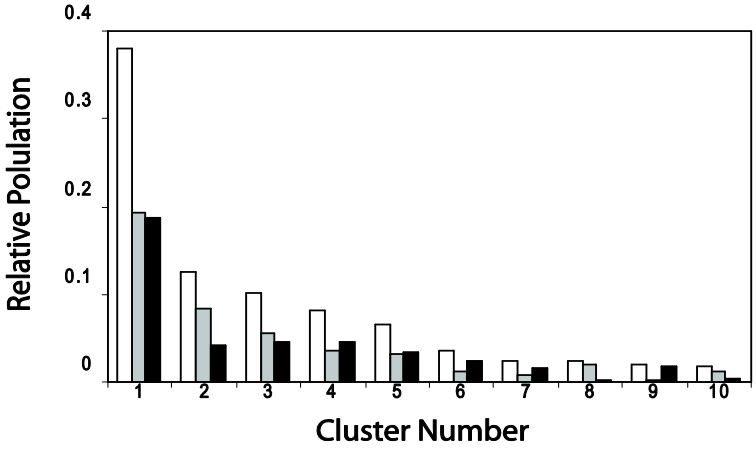

Figure 5.6 The relative population of the top 10 clusters of the whole 4500 peptide configurations which equally obtained from either the simulation of isolated peptide VFVVFV (system IV, 2250 configurations) or a 6×6 array of VFVVFV+PEG-30 (system XII, 2250 configurations). The white columns show the relative population of each cluster (calculated from the total 4500 peptide configurations). The grey columns show in each cluster (in white), the radio of configurations was taken from the simulation of isolated peptide (system IV). The black columns show in each cluster (in white), the radio of configurations was taken from the simulation of a 6×6 array of VFVVFV+PEG-30 (system XII). 0.1 nm cutoff was used for the cluster partition.

The predominant structure in aqueous solution of the acidic EEGEEG peptide is shown in Figure 5.7. The isolated peptide (system VI) primarily adopted a compact random coil conformation (a), whereby the N-terminus (NH_3^+) interacted electrostatically with the COO^- group of one of the Glu residues. Figure 5.7 (b) shows the conformations sampled of an array of EEGEEG+PEG-30 (system XIV). Here the high packing density of the charged peptides affected the electrostatic interaction between the N-terminus (NH_3^+) and the COO^- group at the same chain, producing an extended conformation.

Table 5.2 An overview of the results of cluster analysis.

Compared systems	Side chain type	Correlation coefficient
II and X	-	0.96
II and XI	-	0.93
IV and XII	Non polar	0.95
V and XIII	Polar	0.73
VI and XIV	Negative charge	0.32
VII and XV	Positive charge	0.64

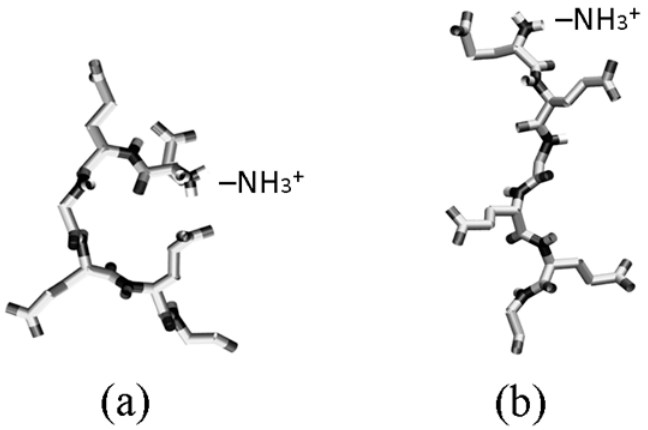

Figure 5.7 The predominant structure in the solution for the EEGEEG peptide. (a) Free peptide in aqueous solution (system VI). (b) Conformation of peptides in a 6×6 array of EEGEEG+PEG-30 (system XIV)

5.4 Conclusions.

Using molecular dynamics (MD) simulation techniques, we have investigated the influence of the PEG spacer on the conformation properties of the peptides to which it is attached. Experimental studies on the short chain PEG, and its analogue poly(ethylene oxide), indicate they form helices in aqueous solution. Molecular dynamics simulations using the forcefield of Anderson and Wilson [23], parameterized for poly(ethylene oxide) demonstrate PEG-10 also adopt a helical conformation, both isolated in solution and covalently bound to a peptide in a 2D array. Here, a series of five peptides with differing physical-chemical properties have been examined. Cluster analysis showed for the specific epitope, polar and nonpolar peptide, there was a high correlation between the configurations sampled by the isolated peptide and the PEGylated peptide, demonstrating that, the conformation of the electrostatically neutral test peptides remains relatively unchanged by PEGylation. For the charged peptides, both negative and positive, a low correlation has been found between the configurations sampled by the isolated peptide and the PEGylated peptide. This may due to high packing density of the charged residues affect the electrostatic interactions of the attached peptide, producing a more extended peptide conformation in the PEGylated peptides. The attached peptides readily interacted at the average experimentally determined high packing density. This suggests that the high packing densities might have a more significant effect on the availably of peptide than the effect of the PEG spacer.

References

1. van Gunsteren, W.F., X. Daura, and A.E. Mark, *Computation of free energy.* Helvetica Chimica Acta, 2002, **85**, 3113-3129.
2. Milton Harris, J. and R.B. Chess, *Effect of PEGylation on pharmaceuticals.* Nature Reviews Drug Discovery, 2003, **2**, 214-221.
3. Milton Harris, J., *Poly(ethylene glycol) chemistry: biotechnical and biomedical applications (topics in applied chemistry).* Springer, 1992.
4. Davis, F.F., *Enzyme polyethylene glycol adducts: Modified enzymes with unique properties.* Enzyme Eng., 1978, **4**, 169-173.
5. Veronese, F.M. and G. Pasut, *PEGylation, successful approach to drug delivery.* Drug Discovery Today, 2005, **10**, 1451-1458.
6. Kozlowski, A. and J. Milton Harris, *Improvements in protein PEGylation: Pegylated interferons for treatment of hepatitis C.* Journal of Controlled Release, 2001, **72**, 217-224.
7. Elbert, D.L. and J.A. Hubbell, *Surface treatments of polymers for biocompatibility.* Annual Review of Materials Science, 1996, **26**, 365-394.
8. Amiji, M. and K. Park, *Surface modification of polymeric biomaterials with poly(ethylene oxide), albumin, and heparin for reduced thrombogenicity.* Journal of biomaterials science. Polymer edition, 1993, **4**, 217-234.
9. Jeon, S.I., J.H. Lee, J.D. Andrade, and P.G. De Gennes, *Protein-surface interactions in the presence of polyethylene oxide. I. Simplified theory.* Journal of Colloid And Interface Science, 1991, **142**, 149-158.
10. Arakawa, T. and S.N. Timasheff, *Mechanism of poly(ethylene glycol) interaction with proteins.* Biochemistry, 1985, **24**, 6756-6762.
11. Hermans, J., *Excluded-volume theory of polymer-protein interactions based on polymer chain statistics.* The Journal of Chemical Physics, 1982, **77**, 2193-2203.
12. Morar, A.S., J.L. Schrimsher, and M.D. Chavez, *PEGylation of proteins: A structural approach.* BioPharm International, 2006, **19**, 34-49.
13. Fee, C.J. and J.M. Van Alstine, *PEG-proteins: Reaction engineering and separation issues.* Chemical Engineering Science, 2006, **61**, 934-939.
14. Veronese, F.M. and J.M. Harris, *Introduction and overview of peptide and protein pegylation.* Advanced Drug Delivery Reviews, 2002, **54**, 453-456.
15. Katre, N.V., *The conjugation of proteins with polyethylene glycol and other polymers. Altering properties of proteins to enhance their therapeutic potential.* Advanced Drug Delivery Reviews, 1993, **10**, 91-114.
16. Nolan, J.P., S. Lauer, E.R. Prossnitz, and L.A. Sklar, *Flow cytometry: A versatile tool for all phases of drug discovery.* Drug Discovery Today, 1999, **4**, 173-180.
17. Miller, C.R., R. Vogel, P.P.T. Surawski, S.R. Corrie, A. RuÌˆhmann, and M. Trau, *Biomolecular screening with novel organosilica microspheres.* Chemical Communications, 20054783-4785.
18. Miller, C.R., R. Vogel, P.P.T. Surawski, K.S. Jack, S.R. Corrie, and M. Trau, *Functionalized organosilica microspheres via a novel emulsion-based route.* Langmuir, 2005, **21**, 9733-9740.
19. Battersby, B.J. and M. Trau, *Novel miniaturized systems in high-throughput screening.* Trends in Biotechnology, 2002, **20**, 167-173.
20. Lindahl, E., B. Hess, and D. van der Spoel, *GROMACS 3.0: A package for molecular simulation and trajectory analysis.* Journal of Molecular Modeling,

2001, **7**, 306-317.
21. Spoel, D.v.d., E. Lindahl, and B. Hess, *GROMACS User Manual version 3.2.* University of Groningen, the Netherlands, 2004.
22. Oostenbrink, C., A. Villa, A.E. Mark, and W.F. van Gunsteren, *A biomolecular force field based on the free enthalpy of hydration and solvation: The GROMOS force-field parameter sets 53A5 and 53A6.* Journal of Computational Chemistry, 2004, **25**, 1656-1676.
23. Anderson, P.M. and M.R. Wilson, *Developing a force field for simulation of poly(ethylene oxide) based upon ab initio calculations of 1,2-dimethoxyethane.* Molecular Physics, 2005, **103**, 89-97.
24. Berendsen, H.J.C., J.P.M. Postma, W.F. van Gunsteren, and J. Hermans, *Interaction models for water in relation to protein hydration.* In Intermolecular Forces, Holland, 1981.
25. Tironi, I.G., R. Sperb, P.E. Smith, and W.F. van Gunsteren, *A generalized reaction field method for molecular dynamics simulations.* The Journal of Chemical Physics, 1995, **102**, 5451-5459.
26. Hess, B., H. Bekker, H.J.C. Berendsen, and J.G.E.M. Fraaije, *LINCS: A linear constraint solver for molecular simulations.* Journal of Computational Chemistry, 1997, **18**, 1463-1472.
27. Miyamoto, S. and P.A. Kollman, *Settle-analytical version of the shake and Rattle algorithm for rigid water models.* Journal of Computational Chemistry, 1992, **13**, 952-962.
28. Feenstra, K.A., B. Hess, and H.J.C. Berendsen, *Improving efficiency of large time-scale molecular dynamics simulations of hydrogen-rich systems.* Journal of Computational Chemistry, 1999, **20**, 786-798.
29. Berendsen, H.J.C., J.P.M. Postma, W.F. van Gunsteren, A. Dinola, and J.R. Haak, *Molecular dynamics with coupling to an external bath.* The Journal of Chemical Physics, 1984, **81**, 3684-3690.
30. Humphrey, W. and A. Dallke, *VMD: Visual molecular dynamics.* J.Mol. Graph., 1996, **14**, 33-38.
31. Daura, X., W.F. van Gunsteren, and A.E. Mark, *Folding-unfolding thermodynamics of α-heptapeptide from equilibrium simulations.* Proteins: Structure, Function and Genetics, 1999, **34**, 269-280.
32. Daura, X., K. Gademann, B. Jaun, D. Seebach, W.F. van Gunsteren, and A.E. Mark, *Peptide folding: When simulation meets experiment.* Angewandte Chemie - International Edition, 1999, **38**, 236-240.
33. Dunbrack Jr, R.L., *Rotamer libraries in the 21st century.* Current Opinion in Structural Biology, 2002, **12**, 431-440.
34. Kabsch, W. and C. Sander, *Dictionary of protein secondary structure: Pattern recognition of hydrogen-bonded and geometrical features.* Biopolymers - Peptide Science Section, 1983, **22**, 2577-2637.
35. Wahab, S.A. and H. Matsuura, *IR spectroscopic study of conformational properties of a short-chain poly(oxyethylene) (C1E3C1) in binary mixtures with liquids of different hydrogen-bonding abilities.* Physical Chemistry Chemical Physics, 2001, **3**, 4689-4695.
36. Oesterhelt, F., M. Rief, and H.E. Gaub, *Single molecule force spectroscopy by AFM indicates helical structure of poly(ethylene-glycol) in water.* New Journal of Physics, 1999, **1**, 6.1-6.11.
37. Tasaki, K., *Poly(oxyethylene)-water interactions: A molecular dynamics study.* Journal of the American Chemical Society, 1996, **118**, 8459-8469.